Regime shifts in a phage-bacterial ecosystem and strategies for its control

Sergei Maslov,[a] Kim Sneppen [b,*]

University of Illinois at Urbana-Champaign, Department of Bioengineering, and Carl R. Woese Institute for Genomic Biology, Urbana, IL 61801, USA[a]; University of Copenhagen, Center for Models of Life, Niels Bohr Institute, 2100 Copenhagen, Denmark [b]

ABSTRACT The competition between bacteria often involves both nutrients and phage predators and may give rise to abrupt regime shifts between the alternative stable states characterized by different species compositions. While such transitions have been previously studied in the context of competition for nutrients, the case of phage-induced bistability between competing bacterial species has not been considered yet. Here we demonstrate a possibility of regime shifts in well-mixed phage-bacterial ecosystems. In one of the bistable states the fast-growing bacteria competitively exclude the slow-growing ones by depleting their common nutrient. Conversely, in the second state the slow-growing bacteria with a large burst size generate such a large phage population that the other species cannot survive. This type of bistability can be realized as the competition between a strain of bacteria protected from phage by abortive infection and another strain with partial resistance to phage. It is often desirable to reliably control the state of microbial ecosystems, yet bistability significantly complicates this task. We discuss successes and limitations of one control strategy in which one adds short pulses to populations of individual species. Our study proposes a new type of phage therapy, where introduction of the phage is supplemented by addition of a partially resistant host bacteria.

IMPORTANCE Phage-microbial communities play an important role in human health as well as natural and industrial environments. Here we show that these communities can assume several alternative species compositions separated by abrupt regime shifts. Our model predicts these regime shifts in the competition between bacterial strains protected by two different phage defense mechanisms: abortive infection/CRISPR and partial resistance. The history dependence caused by regime shifts greatly complicates the task of manipulation and control of a community. We propose and study a successful control strategy via short population pulses aimed at inducing the desired regime shifts. In particular, we predict that a fast-growing pathogen could be eliminated by a combination of its phage and a slower-growing susceptible host.

KEYWORDS: keyword 1, keyword 2, keyword 3.

Please read the Instructions to Authors carefully, or browse the FAQs for further details.

INTRODUCTION

Diverse ecosystems are known to be capable of regime shifts in which they abruptly and irreversibly switch between two mutually exclusive stable states (1). Such regime shifts have been extensively studied in both macroscopic and microbial ecosystems (1) and shown to be hysteretic and history-dependent. In microbial ecosystems (2) these

transitions are known to be possible when a bacterial species directly produces some metabolic waste products or antibiotics (3) that inhibit the growth of other bacteria. They may also occur when bacterial species compete for several food sources, which they use either in different stoichiometric ratios (4) or in different preferential orders (5). Here we explore a new type of regime shifts caused by interactions between bacteria and phages. Bacteriophages have long been known to increase bacterial diversity, especially in aquatic environments (6, 7). However, their potential to create multiple stable states with distinct bacterial species compositions so far has not been recognized. Here we illustrate a possibility of such alternative stable states and regime shifts using a computational model in which two bacterial species compete for the same food source, and are simultaneously exposed to an infection by the same virulent phage. Such dual constraints are known to abate the usual competitive exclusion (8) by allowing multiple bacterial species consuming the same nutrient to co-exist (9, 7).

Microbial communities are an important part of our natural and artificial surroundings and are also responsible for many aspects of human health. Some compositions of microbial communities may be useful for us, while other might be detrimental or even lethal. Thus we would like to reliably manipulate and control the species compositions of these systems. Here we explore several strategies aimed to control the state of phage-bacterial ecosystems via short population pulses inducing the desired regime shift.

MODEL AND RESULTS

Model We study a model describing the dynamics of two microbial species with populations B_1 and B_2 growing on a single limiting nutrient (e.g. carbon source) with concentration C and infected by a single phage species with population P. All populations are assumed to be well-mixed in an environment constantly supplied with the limiting nutrient at a rate ϕ. The dynamics of this ecosystem is given by

$$\frac{dC}{dt} = \phi - C \cdot \delta_C - C \cdot \left(\frac{\lambda_1}{Y_1} B_1 + \frac{\lambda_2}{Y_2} B_2 \right) \tag{1}$$

$$\frac{dB_1}{dt} = B_1 \cdot (\lambda_1 C - \eta_1 P - \delta_B) \tag{2}$$

$$\frac{dB_2}{dt} = B_2 \cdot (\lambda_2 C - \eta_2 P - \delta_B) \tag{3}$$

$$\frac{dP}{dt} = P \cdot (\beta_1 \eta_1 B_1 + \beta_2 \eta_2 B_2 - \delta_P) \tag{4}$$

The growth rate of each bacterial species is assumed to be proportional to the nutrient concentration C with the species B_1 growing faster than the species B_2: $\lambda_1 > \lambda_2$. Nutrient yields of these two species are given by Y_1 and Y_2 respectively. Phage adsorption coefficients of two species are given by η_1 and η_2 and their burst sizes are β_1 and β_2. The two bacterial species in our model are assumed to have the same death rate δ_B that also includes possible contribution from dilution of their shared environment. The death/dilution rate of the phage is given by δ_P and the nutrient is diluted at a rate δ_C.

Conditions for bistability and regime shifts In what follows we explore the steady state solutions of Eqs. 1-4, - the only asymptotic dynamical behavior possible in our system. In the absence of phages, the faster growing species B_1 would always eliminate the slower growing species B_2 due to competitive exclusion (8). Phages in principle allow for a slow-growing species to co-exist with the fast-growing one or even to completely take over the ecosystem. In order for this to happen in high-nutrient/high-phage environments the species B_2 needs to be less susceptible to phage infections than the species B_1: $\lambda_1/\eta_1 < \lambda_2/\eta_2$. In the extreme case, where the species B_2 is fully
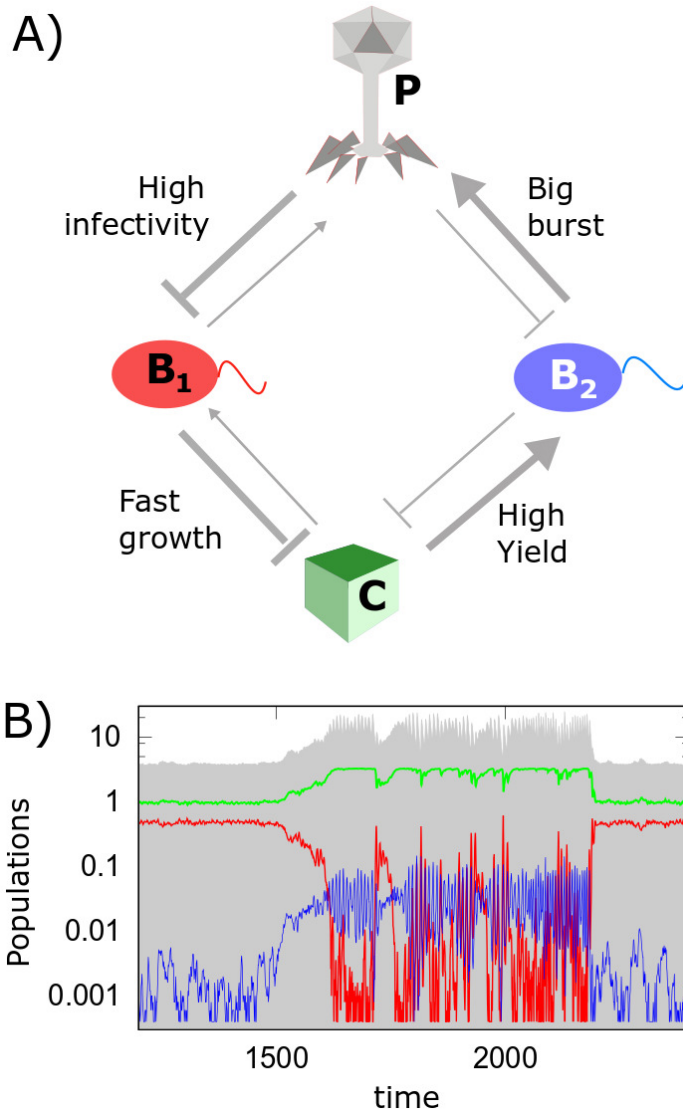
FIG 1 **Alternative stable states and regime shifts in a phage-bacterial ecosystem. A) The diagram of interactions between the three species and one nutrient resource in our model: the fast-growing (red, B_1) and the slow-growing (blue, B_2) bacterial species are limited by the same nutrient C and infected by the same phage P. The slow-growing bacteria are more protected from infections by phage, but, if infected, they generate a larger burst size. The negative effective interaction from B_1 to B_2 is mediated via the nutrient, while that from B_2 to B_1 - via the phage. B) A representative stochastic simulation of the model. Note the abrupt and large regime shifts of the ecosystem between two alternative stable states dominated by bacteria B_1 and B_2 correspondingly. All populations are always maintained above a very low level 4×10^{-4} provided by a weak influx of species to the ecosystem. Both phage and nutrient concentrations experience a discontinuous shift up if the ecosystem suddenly flips from the B_1-dominated state to the B_2-dominated one and down in the opposite case. The model parameters are $\lambda_1 = 1$, $\lambda_2 = 0.8$, $Y_1 = Y_2 = 1$, $\eta_1 = 0.20$, $\eta_2 = 0.15$, $\beta_1 = 2$, $\beta_2 = 40$, $\delta_C = \delta_B = \delta_P = 0.2$ and $\phi = 0.66$.**

resistant to the phage ($\eta_2 = 0$), the co-existence between these bacterial species has been previously identified and computationally studied (9, 7, 10).

Here we introduce and study another regime of a phage-bacterial ecosystem in which two bacterial species could mutually exclude each other. This falls under the category of discontinuous and abrupt regime shifts between alternative stable states in microbial ecosystems (see Ref. (2) for a review), which have been previously modelled in the context of competition for nutrients (5, 4) and without phages. In order for a phage-bacterial ecosystem to be in principle capable of bistability, the slow-growing bacterial species needs to produce disproportionately more phages per each unit of consumed nutrient than the fast-growing one: $Y_2\beta_2 > Y_1\beta_1$. As we show in the Supplementary Materials, the bistability requires the following three inequalities to be satisfied:

$$\lambda_1 > \lambda_2 \tag{5}$$

$$\frac{\lambda_1}{\eta_1} < \frac{\lambda_2}{\eta_2} \tag{6}$$

$$\frac{\lambda_1}{Y_1\beta_1\eta_1} > \frac{\lambda_2}{Y_2\beta_2\eta_2} \tag{7}$$

Figure **??**A illustrates the basic mechanisms responsible for bistability and regime shifts in our ecosystem. The thickness of each arrow scales with the relative strength of the interaction between the nodes it connects. Thus the width of the arrow pointing from the nutrient to the bacterial species B_i reflects its growth rate λ_i, while that of the arrow pointing in the opposite direction - the rate λ_i/Y_i at which this bacterial species depletes the nutrient. Similarly, the width of the arrow pointing from the phage to the bacterial species B_i reflects its adsorption coefficient η_i, while that of the arrow going in the opposite direction - the rate $\beta_i\eta_i$ at which this bacterial species generates new phages.

Figure **??**B shows a stochastic simulation of our model with parameters $\lambda_1 = 1$, $\lambda_2 = 0.8$, $Y_1 = Y_2 = 1$, $\eta_1 = 0.20$, $\eta_2 = 0.15$, $\beta_1 = 2$, $\beta_2 = 40$, $\delta_C = \delta_B = \delta_C = 0.2$ and $\phi = 0.66$ (see Methods for details). In our simulations we do not allow the population of either of three species (B_1, B_2, and P) to fall below a very small value 4×10^{-4}. This is equivalent to keeping a constant but weak influx of these species to the ecosystem. As a result, each species would start growing as soon as ecosystem's internal parameters would make its net growth rate positive.

Random fluctuations in population sizes of bacteria and phages could trigger spontaneous regime shifts between two alternative stable states of the ecosystem visible in Figure **??**B. One of these states is dominated by the fast growing bacterial species B_1. It suppresses the slow-growing species B_2 by the virtue of competitive exclusion via their shared nutrient. In the second stable state the slow-growing species B_2 with a large burst size β_2, generates such a high population of phages that they completely eliminate the fast-growing species B_1, which is relatively more susceptible to phage infections. This steady state also has a larger nutrient concentration due to a slower rate of its depletion by the species B_2.

History dependence of the ecosystem state When Eqs. (5-7) are satisfied, the bistability is possible only in a certain intermediate range of the nutrient supply rate. Fig. 2A-D shows the changes in, respectively, steady state values of P, B_1, B_2 and C when the nutrient supply rate ϕ is slowly changed first up from 0 to 1 and then down to 0 again. For very low nutrient supply rates $\phi < 0.04$ neither bacteria nor phages can survive and the system stays abiotic $B_1 = B_2 = P = 0$. The fast-growing bacteria B_1 first appears for $\phi \geq 0.04$ and prevents the appearance of the slow-growing
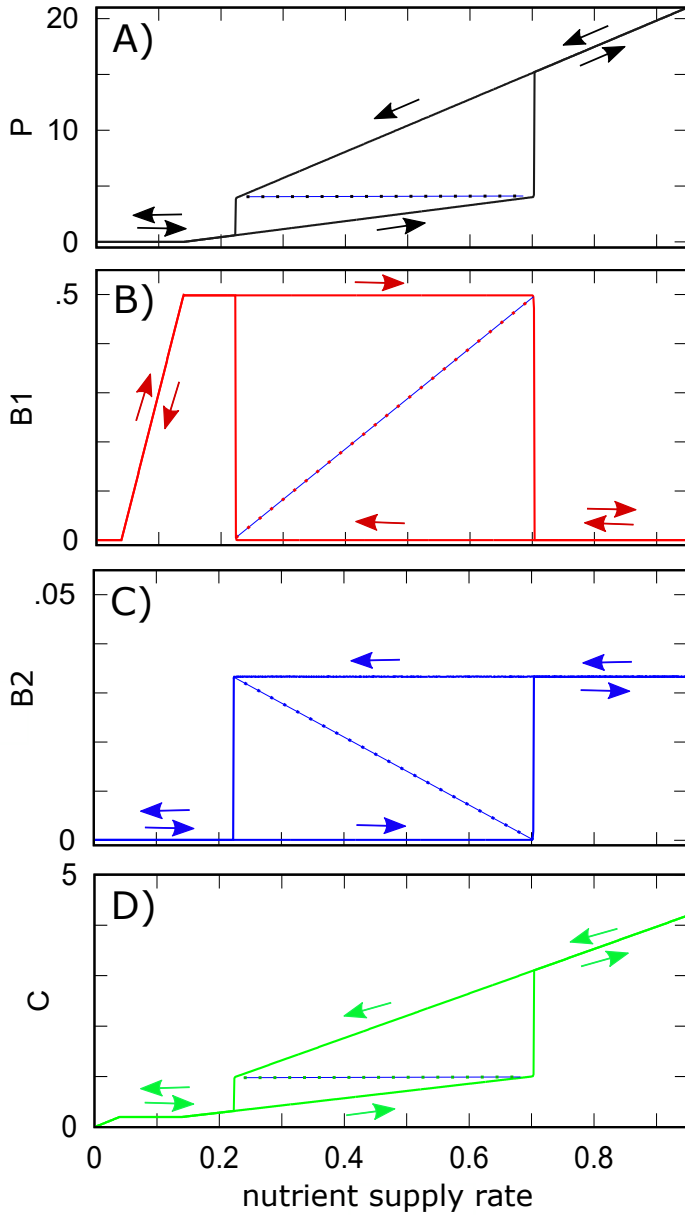
FIG 2 Hysteresis loops in populations of phage P (black), fast-growing bacteria B_1 (red), slow-growing bacteria B_2 (blue) and nutrient concentration C (green) as the nutrient supply rate ϕ (x-axis) is changed first up from 0 to 1 and then down to 0. Note two sudden discontinuous transitions (regime shifts) at both ends of the hysteresis loop. The dashed lines mark populations in the dynamically unstable state separating two alternative stable states. Parameters of the model are the same as in Fig. 1, except for a varying nutrient supply rate ϕ (x-axis) and the absence of stochastic fluctuations.
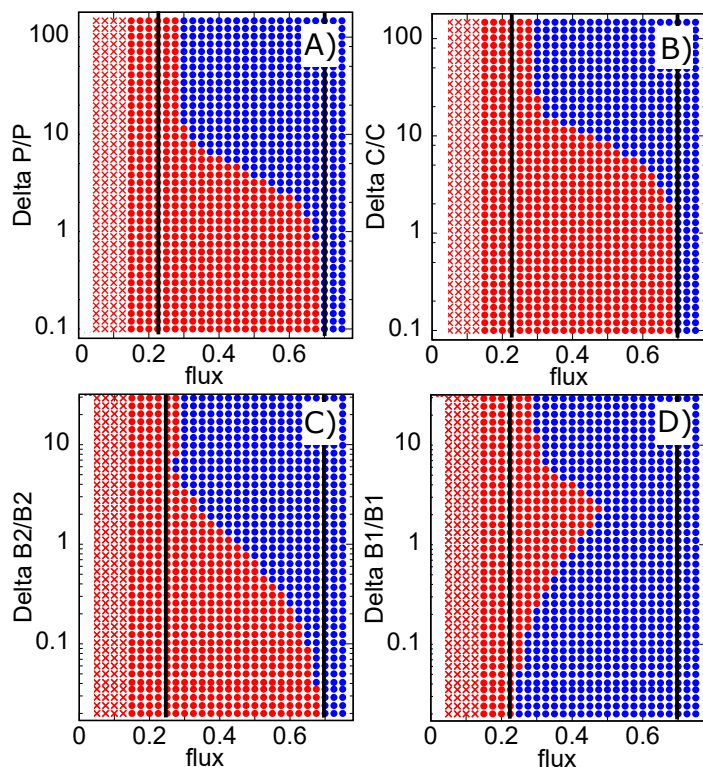
FIG 3 Control of the ecosystem by a pulse in phage population P (panel A), resource concentration C (panel B), bacterial populations B_2 (panel C), or B_1 (panel D). Red symbols mark the B_1-dominated state, while blue symbols - the B_2-dominated state. In the region marked with red crosses phages cannot exist: $P = 0$. The x-axis is the nutrient supply rate ϕ with the bi-stable region confined between two black solid lines. The y-axis is the magnitude of the pulse normalized by the population/concentration of the target stable state, that is to say, by that of the B_2-dominated state in panels A-C and of the B_1-dominated state in panel D. For nutrient supply rates $0.27 < \phi < 0.7$ the B_1-dominated state (red) can be switched to the B_2-dominated state (red) by adding a sufficiently large pulse of phage P (panel A), nutrient C (panel B), or bacteria B_2 (panel C). Conversely, for $0.23 < \phi < 0.46$ the B_2-dominated state (blue) can be switched to the B_1-dominated state (red) by adding a sufficiently large pulse of bacteria B_1 (panel D).

species due to competitive exclusion. As the nutrient supply rate is increased above 0.14, the population of the phage P becomes sustainable and linearly increases with ϕ. B_2 continues to be competitively excluded until much higher rate of nutrient supply $\phi^{(1)} = 0.70$, at which the ecosystem undergoes a regime shift to the state dominated by B_2 and excluding B_1. This alternative stable state persists all the way up the nutrient supply rate. The growth of B_1 is prevented by a high phage population to which this species is especially susceptible. When ϕ is lowered, the B_2-dominated state survives down to the nutrient supply rate $\phi^{(2)} = 0.23$, which is much lower than $\phi^{(1)} = 0.70$. Thus for nutrient supply rates between 0.23 and 0.70 the ecosystem is bistable and can be in any of the two alternative stable states making upper and lower parts of the hysteresis loops in Fig. 2A-D. Note that the population of phages and the concentration nutrients generally change in synchrony: when B_1 is dominant, both phage and nutrient levels are low, while the dominance of B_2 generates many phages which significantly lower its population and prevent it from fully exploiting resources, thereby keeping C high.

Controlling regime shifts by population pulses Phages have recently been investigated as potential agents of control of populations of individual bacterial species in the gut microbiome (11). However, when alternative stable states are present, the state of an ecosystem is complicated by hysteresis and history dependence.

One may need to switch a microbial ecosystem from an undesirable/diseased state to a desirable/healthy state without perturbing the environmental parameters such as nutrient supply rate. One way to achieve such control is by adding a fixed amount of one of the species P, B_1, B_2, or of the nutrient C giving rise to an instantaneous increase of its current population/concentration. Such one-time addition, which we call a "population pulse", is similar to the "impulsive control strategy" discussed in Ref. (12). Since P, C, and B_2 are all higher in the B_2-dominated state than in the B_2-dominated state, adding a population pulse of either one of them to the B_1-dominated state could, in principle, trigger a regime shift. Similarly, adding a population pulse of B_1 to the B_2-dominated state could result in a regime shift in the opposite direction.

Fig. 3 explores successes and limitations of the population pulse strategy. We found that this strategy works but only within a certain range of nutrient supply that is generally more narrow than the bistability region itself. A regime shift from the B_1- to the B_2-dominated state can be triggered across the entire bistability region. Conversely, a regime shift from the B_2- to the B_1-dominated state by adding a pulse of B_1 can be made only for ϕ below 0.46, which is lower than $\phi^{(1)} = 0.7$ - the upper bound of the bistable region (the right solid line in Fig. 3). Another observation is the reentrant transition in Fig. 3D: adding too much of B_1 to the B_2-dominated state may prevent the regime shift from taking place. We also note that in order to trigger a regime shift one generally needs to add a pulse that would transiently make the population of the perturbed species to exceed its steady state value in the targeted state (pulse normalized to 1 on the y-axis in Fig. 3). Indeed, a pulse changes only one out of four populations/concentrations in our ecosystem. Thus it needs to be large enough to drive the remaining three populations in the general direction of the regime shift.

Consider a situation where we can simultaneously perturb all three species and the nutrient and set their populations/concentrations (C, B_1, B_2, and P) to any desired value. In this case, transient populations after a pulse could be made smaller than their steady state values in the target state. Indeed, to switch the state of the ecosystem, it would be sufficient to make all four populations/concentrations just a little bit closer to the target state than their values in the dynamically unstable state shown as dashed lines in Fig. 2A-D.

Model with perfect abortive infection in B_1 In one of the phage defense mechanisms called abortive infection (Abi) (13) phages enter and kill the host without producing any phage progeny. A special limit of our model is obtained when the species B_1 is characterized by abortive infection: $\beta_1 = 0$, while $\eta_1 > 0$. Our equations in this case predict $\phi^{(1)} = \infty$, which means that B_1 would not disappear from the ecosystem for any nutrient supply ϕ. Indeed, this species generates no phage progeny, thus it always can outcompete a small amount of the slower-growing species B_2 infected by phages. However, analogous to Fig. 3A,C a sufficiently large population pulse of B_2 and P can get established in the system and eliminate B_1. This could happen for $\phi > \phi^{(2)}$.

DISCUSSION

We introduced a mathematical model of regime shifts in phage-bacterial ecosystems. The alternative stable states in our model are populated by different bacterial species mutually excluding each other. The negative interactions between these species are mediated by either their co-infecting phages or their shared nutrients. In this respect the mechanism of bistability in our model is similar to that in consumer resource models without phages (4). Indeed, the mandatory (but not sufficient) condition for bistability in either of these two models is a significant difference in stoichiometry of competing microbial species. In our model this stoichiometry is quantified by $Y \cdot \beta$

Maslov et al.

201 - the product of nutrient yield and burst size of a given bacterial species. It can be
202 interpreted as the conversion factor connecting the amount of nutrients used to build
203 a single bacterial cell to the number phages it produced upon lysis. Comparison of
204 inequalities in Eq. 6 and Eq. 7 shows that bistability is possible only when conversion
205 factors of two bacterial species are sufficiently different from each other: $Y_2 \cdot \beta_2 > Y_1 \cdot \beta_1$.
206 Similarly, multistability studied in Refs. (14, 4) requires species competing for two
207 types of essential resources (e.g. C and N) to have different C:N stoichiometries.
208 Regime shifts and multistability are known to occur when competition between
209 species in principle allows for their co-existence, while the differences in stoichiometry
210 make such coexistence dynamically unstable (14, 4). This is also true in our model,
211 where bistability between species B_1 and B_2 is possible whenever their co-existence
212 is dynamically unstable. Conversely, a dynamically stable co-existence of B_1 and B_2 is
213 possible whenever inequalities given by Eqs 5-6 are satisfied, while that in the Eq. 7
214 changes the direction to $\lambda_1/(Y_1\beta_1\eta_1) < \lambda_2/(Y_2\beta_2\eta_2)$.
215 Our model predicts that regime shifts in phage-microbial ecosystems can be a
216 consequence of differences in species' yields $Y_2 > Y_1$ rather than their burst sizes. A
217 negative correlation between species' growth rate and its yield known as rate-yield
218 trade-off is widely known (15). According to this correlation slower growing species
219 tend to have higher yields thereby facilitating bistability in our model.
220 A general case of predator-prey food webs with multiple trophic levels has been
221 considered in Ref. (16, 17). For certain combinations of parameters one can prove that
222 the steady state of dynamical equations describing such ecosystems is unique and thus
223 multistability is impossible. This proof, based on the Lyapunov function proposed in
224 Ref. (18), requires the food web to have identical stoichiometry products (like $Y_i\beta_i$ in our
225 model) for all paths connecting the same pair of species. Here we extend this study by
226 showing that if the difference in stoichiometries of two such paths is sufficiently large,
227 multistability could in principle emerge. Thus, it is tempting to extend our mechanism
228 for multistability up from microscopic phage-bacterial ecosystems to macroscopic
229 predator-prey food webs. In order for macroscopic food webs to be multistable, the
230 biomass conversion ratio between two successive trophic levels has to deviate widely
231 from its typical value of about 10% (19, 20) and be sufficiently different for different
232 species in the same trophic level. Indeed, one could always choose to measure the
233 population of each species in units of its biomass per unit area. These units would
234 rescale absolute values of competition parameters such as λ and η. In these units
235 stoichiometric coefficients Y and β are given by the efficiency (0%-100%) of biomass
236 conversion between two consecutive trophic levels. Multistability requires sufficient
237 differences in biomass conversion factors along paths between species in different
238 trophic levels. For example, in our model the nutrient, which can be thought to occupy
239 the trophic level 0 is connected to the phage species (trophic level 2) via paths going
240 through two different bacterial species (intermediate trophic level 1). Furthermore,
241 the number of species in intermediate trophic levels of these paths has to be odd.
242 Given that the overall number of trophic levels rarely exceeds 4, the case of a single
243 intermediate trophic level considered in this study represents the most biologically
244 plausible scenario.
245 The ecosystem used in our study is very simple: it has low species diversity and a
246 single growth-limiting nutrient. This simplicity allowed us to quantitatively understand
247 the principal mechanisms giving rise to bistability. More complex ecosystems with a
248 larger number of species and multiple nutrients are expected to have qualitatively
249 similar properties. They also could have a much more complicated phase diagram
250 in the space of nutrient supply rates. Hence multistability with more than two stable

8

251 states could be realized in some regions of this space (See Ref. (4) for this type
252 of multistability in consumer resource models). Another limitation of our model is
253 that it ignores the possibility of rapid evolution of bacterial strains competing with
254 phages. Such red queen dynamics often generates phage-resistant bacterial strains.
255 The appearance of a phage-resistant variant of B_1 would modify the behavior of our
256 ecosystem for very high nutrient supply, but might not affect bistability between B_1 and
257 B_2 for intermediate nutrient supply studied above. This depends on the magnitude of
258 the growth deficiency of the resistant mutant. A delicate interplay between multiple
259 strains and species could be understood by visualizing them all in Fig. 4A, where a
260 phage-resistant strain would be shown as a vertical line.

261 It is instructive to compare the mechanisms of bistability in our model to two
262 previously described bistable systems involving phages and bacteria. One example of
263 alternative stable states in a phage-microbial ecosystem has been described in Ref. (21).
264 Unlike in our model, where regime shifts change the composition of bacterial species,
265 the ecosystem modeled in Ref. (21) switches between the states with and without
266 phages. The main feature responsible for this switching behaviour is a decrease of
267 adsorption coefficient of the bacterial host when nutrients become scarce. Similar to
268 regime shifts in our ecosystem, the feedback between the nutrient concentration and
269 the abundance of phages is at the core of this bistable behavior.

270 Perhaps the most celebrated example of a bistable system is the genetic switch
271 operating inside a bacterial host of a temperate phage (22, 23). In a host of the
272 prophage λ there is an intracellular competition between the dormant, lysogenic state
273 dominated by the repressor protein C1 (24), and the virulent, lytic state dominated
274 by the protein Cro (25). When Cro wins, it leads to production of a large number of
275 phages, akin to the species B_2 in our microbial ecosystem. High nutrient concentration
276 in the environment typically favors the lytic state of the λ-host (26). Such lytic state is
277 analogous to the B_2-dominated regime in our ecosystem, also favored by high C. In
278 this sense our ecosystem can be in the "dormant state" producing few phages when it
279 is dominated by B_1. When this state is exposed to a strong pulse of P, C, or B_2 it can
280 switch to the "lytic state" dominated by B_2 and producing many phages (see Fig. 3).

281 One realistic implementation of bistability predicted by our model is in a phage-
282 microbial ecosystem consisting of a bacterial strain protected against phages by the
283 abortive infection (Abi) mechanism (B_1) and a partially-resistant strain (B_2) co-infected
284 by the same phage. Hosts with abortive infection allow phages to enter and kill them
285 without producing a noticeable phage progeny (13). An example of the Abi defense
286 is provided by certain types of CRISPR defense (27, 28, 29), where phages kill most of
287 infected hosts but have zero or small burst size. In contrast to Abi- or CRISPR-protected
288 bacteria, partially resistant strains may arise due to a mutation in the receptor protein
289 which reduces both the growth rate (30) and the phage adsorption but has little effect
290 on the burst size. Thus regime shifts may naturally occur as a consequence of diverse
291 phage defence mechanisms in microbial ecosystems (31).

292 A potential application of our system is in a new type of phage therapy in which
293 phages targeting the pathogenic species (B_1) are introduced together with carefully
294 selected non-pathogenic species (B_2) infected by the same phage. This therapy effec-
295 tively combining two population pulses shown in panels A and C of Fig. 3 would lead to
296 a more efficient and permanent elimination of the fast-growing pathogen (B_1). One
297 of the advantages of this approach is that phages would be continually present in the
298 former patient thereby preventing reentry of pathogenic bacteria. The strategy could
299 be made even more favourable if the bacteria added together with phages would use
300 a nutrient other than C rendering it not vulnerable to nutrient competition from the

Maslov et al.

301   pathogen.

METHODS

303   **Simulations** The paper investigates the dynamics of a model defined by Eqs. (1-4),
304 built on assumptions of mass action kinetics in a well-mixed system with an adjustable
305 nutrient supply rate (32). We performed both deterministic and stochastic simulations
306 of this model.

307   In stochastic simulations shown in Fig. 1B we use the Gillespie algorithm with step
308 size of 0.0002 and rates defined for each of the 9 basic processes in Eqs 1-4: nutrient
309 introduction and dilution events, B_1 and B_2 replication events, phage infection events
310 separately in B_1 and in B_2, and combined death/decay/dilution events in each of the
311 two bacteria and one phage species. Notice that a single phage infection event reduces
312 the bacterial population by the step size equal to 0.0002, but increases the phage
313 population by $\beta \cdot 0.0002$. A large value of the burst size $\beta_2 = 40$ justifies a small step size
314 used in our simulations.

315   Deterministic simulations shown in Fig. 2 solve the dynamics given by Eqs. (1-
316 4). At each value of nutrient supply rate ϕ we integrate the equations for 1000 time
317 units to eliminate transients. We then increase the nutrient supply rate in increments
318 $\Delta\phi = 0.01$. We use the steady state populations/concentrations obtained at ϕ as
319 starting populations/concentrations for simulations at $\phi + \Delta\phi$.

320   Each blue or red dot in Fig. 3 was obtained by starting the system in one of
321 the stable states, and subsequently changing one of the variables (P, C, B_1 or B_2) as
322 indicated on the y-axis. After a deterministic simulation of dynamical Eqs. (1-4) for
323 1000 time-units, the final state is compared to each of the states possible for a given
324 value of ϕ and is marked with the corresponding color Fig. 3.

325   **Conditions for bistability** In our model it is convenient to describe the growth of a
326 microbial species in (C, P) coordinates, characterizing respectively the nutrient and the
327 phage concentrations in the environment. The population of a species exponentially
328 grows for $\lambda C - \eta P > \delta_B$, exponentially decays for $\lambda C - \eta P < \delta_B$, and stays constant for
329 $\lambda C - \eta P = \delta_B$. The last equation defines the so-called Zero Net Growth Isocline (ZNGI)
330 (14) of the species defined by all environmental parameters where the population of
331 this species could be in a steady state. Everywhere in the region of the (C, P)-plane
332 located to the right and below of species ZNGI (high C and small P) its population
333 exponentially grows, while in the region to the left and above its ZNGI (low C and large
334 P) it exponentially decays.

335   Red and blue straight lines in Fig. 4A correspond to the Zero Net Growth Isoclines
336 (ZNGI) of, correspondingly, the fast- and the slow-growing bacterial species in our
337 model. They intersect at the point (C^*, P^*) given by

$$C^* = \frac{\delta_B \cdot (\eta_1 - \eta_2)}{\lambda_1 \lambda_2 \cdot \left(\frac{\eta_1}{\lambda_1} - \frac{\eta_2}{\lambda_2}\right)} \tag{8}$$

$$P^* = \frac{\delta_B \cdot (\lambda_1 - \lambda_2)}{\lambda_1 \lambda_2 \cdot \left(\frac{\eta_1}{\lambda_1} - \frac{\eta_2}{\lambda_2}\right)} \tag{9}$$

340 The intersection point correspond to the only set of environmental parameters at
341 which these two species can potentially coexist with each other.

342   The lower part of the species 1 ZNGI (the solid part of the red line) extending from
343 $P = 0$ and up to the intersection point at P^* and the upper part of the species 2 ZNGI
344 above P^* (the solid part of the blue line) have a special property that the other species
345 would not be able to grow in this environment. Hence, the union of these two halves
346 of ZNGIs corresponds to uninvadable states of the ecosystem, which are the main
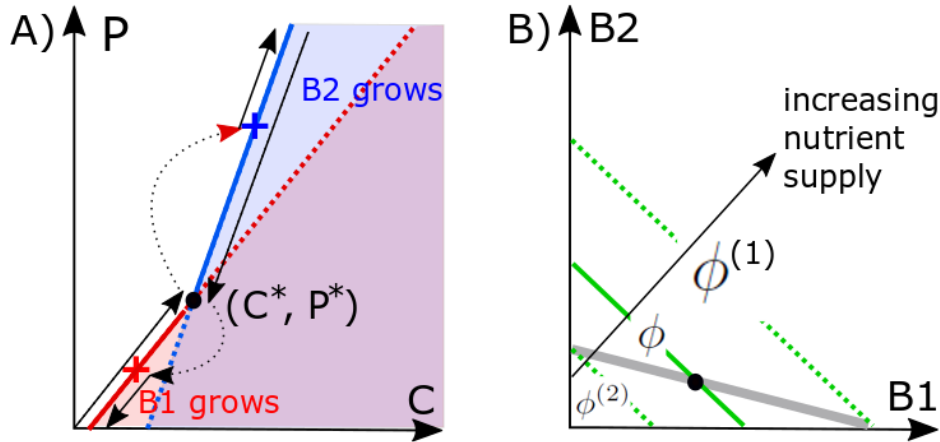
FIG 4 **Geometric solution of the steady state of the ecosystem. A) Steady state C and P are from solving Eqs. (2-3). When both bacteria B_1 and B_2 are present the system can only be at the intersection $(C^*, P*)$. In our case this state is dynamically unstable. As ϕ increases, the environmental parameters (C, P) follow the solid red line up to the black dot, then discontinuously jumps to the blue cross and continues up along the solid blue line. When ϕ subsequently decreases in the hysteresis loop shown in Fig. 2, the (C, P) follow the solid blue line down to the black dot, discontinuously jumps to the red cross and continues down along the solid red line. This trajectory is shown in black lines with arrows. B) The geometric solution for coexisting bacterial populations is given by the intersection of the grey line, where the phage population is at the steady state $P = P^*$ (Eq. 14), and the green line, where the nutrient concentration is at the steady state $C = C^*$ (Eq. 15). The green line shifts up as the nutrient supply ϕ is increased. Bacterial populations B_1 (B_2) disappear at the boundaries $\phi^{(1)}$ ($\phi^{(2)}$) of the bistability region $\phi^{(2)} < \phi < \phi^{(1)}$. Here we show an example in which the steady state C^*, P^* is dynamically unstable giving rise to bistability. However, if the grey line has a steeper slope than the green line, the bistability is replaced by the region ($\phi^{(1)} < \phi < \phi^{(2)}$) of stable coexistence of B_1 and B_2.**

focus of this study. The exact position of the environmental parameters on the (C, P) plane is determined by the supply rate ϕ of the limiting nutrient to the ecosystem. For $\phi < \delta_C \delta_B / \lambda_1$ there is not enough nutrient to support the growth of any species and the environment remains abiotic. Hence the first transition happens at

$$\phi_{B1} = \frac{\delta_C \delta_B}{\lambda_1} \quad . \tag{10}$$

For $\phi_{B1} < \phi < \delta_C \delta_B / \lambda_1 + \delta_P \delta_B / (Y_1 \beta_1 \eta_1)$, the species 1 is present but its biomass is not sufficient to support the survival of the phage. The phage first enters the ecosystem at

$$\phi_{P1} = \frac{\delta_C \delta_B}{\lambda_1} \cdot \left(1 + \frac{\delta_P}{\delta_C} \cdot \frac{\lambda_1}{Y_1 \beta_1 \eta_1}\right) \quad . \tag{11}$$

For even larger nutrient supply rates: $\phi_{P1} < \phi < \phi^{(1)} = C^* \delta_P \left(\frac{\lambda_1}{Y_1 \beta_1 \eta_1} + \frac{\delta_C}{\delta_P}\right)$ the ecosystem contains only the species 1 and the phage. The crucial parameters of the phage-bacterial ecosystem considered in our model are

$$\phi^{(1)} = C^* \delta_P \left(\frac{\lambda_1}{Y_1 \beta_1 \eta_1} + \frac{\delta_C}{\delta_P}\right) \tag{12}$$

$$\phi^{(2)} = C^* \delta_P \left(\frac{\lambda_2}{Y_2 \beta_2 \eta_{2}} + \frac{\delta_C}{\delta_P}\right) \quad , \tag{13}$$

where C^* is given by the Eq. 8. For nutrient supply rates $\phi > \phi^{(1)}$ the species 2 can in principle grow in the ecosystem give C and P shaped by the species 1. What happens

in this region crucially depends on whether $\phi^{(1)} < \phi^{(2)}$ or $\phi^{(1)} > \phi^{(2)}$, with the latter case corresponding to bistability which is the main focus of this study. For pedagogical reasons, let us first consider the model where $\phi^{(1)} < \phi^{(2)}$ and thus B_1-B_2 co-existence is possible. In this case both species 1 and 2 can co-exist with each other in the interval $C^* \delta_P \left(\frac{\lambda_1}{Y_1 \beta_1 \eta_1} + \frac{\delta_C}{\delta_P} \right) = \phi^{(1)} < \phi < \phi^{(2)} = C^* \delta_P \left(\frac{\lambda_2}{Y_2 \beta_2 \eta_2} + \frac{\delta_C}{\delta_P} \right)$. The abundances of each of the two microbial species can be geometrically determined as the intersection of two straight lines in the (B_1, B_2)-plane shown in Fig. 4B. The grey line corresponds to the steady state of the phage population P in Eq. 4 and is given by the equation

$$\beta_1 \eta_1 B_1 + \beta_2 \eta_2 B_2 = \delta_P \qquad . \tag{14}$$

It must intersect with another straight line defining the steady state of the nutrient concentration $C = C^*$ and is given by

$$\frac{\lambda_1 B_1}{Y_1} + \frac{\lambda_2 B_2}{Y_2} = \frac{\phi}{C^*} - \delta_C \qquad . \tag{15}$$

These lines intersect for positive B_1 and B_2 when $\phi^{(1)} < \phi < \phi^{(2)}$.

In the opposite case, where $\phi^{(1)} > \phi^{(2)}$, the system is capable of bistability for nutrient supply rates $\phi^{(2)} < \phi < \phi^{(1)}$. To understand this it is useful to follow the trajectory of environmental parameters (C, P) as ϕ is gradually increased. For $\phi_{P1} < \phi < \phi^{(1)}$ the environmental parameters follow the ZNGI of the fast growing species 1 (the red line in Fig. 4A below the intersection with the blue line). Immediately above the intersection point (C^*, P^*), realized for nutrient supply rate slightly larger than $\phi^{(1)}$, the ecosystem becomes invadable by the species 2. However, for this species the intersection point (C^*, P^*) corresponds to a lower value of nutrient supply $\phi^{(2)} < \phi^{(1)}$. Hence after a brief transient period the environmental parameters (C, P) of our ecosystems move to the position marked with the blue cross in Fig. 4A. As ϕ continues to increase above $\phi^{(1)}$, the environmental parameters follow the ZNGI of the species 2 (the blue line to the right of the blue cross in Fig. 4A).

If at some point one starts decreasing ϕ, the species 2 will persist down to $\phi^{(2)}$ at which the environmental parameters are again at the coexistence point (C^*, P^*). For slightly lower ϕ the environmental parameters will discontinuously jump to the point marked with the red cross on the ZNGI of the species 1. For even lower nutrient supply rates they will continue to follow the ZNGI of the species 1 to the left and below of the red cross. Hence, our environment is bistable in the interval of two ZNGIs between the red and blue crosses. The lower red part of this interval is reachable only when ϕ is increased from a low value below $\phi^{(2)}$, while the upper blue part - when ϕ is decreased from a high value above $\phi^{(1)}$.

Above we assumed that phages can survive for $\phi = \phi^{(2)}$ in the ecosystem dominated by the species 1 instead of species 2. This requires $C^* \delta_P \left(\frac{\lambda_2}{Y_2 \beta_2 \eta_2} + \frac{\delta_C}{\delta_P} \right) = \phi^{(2)} > \phi_{P1} = \frac{\delta_C \delta_B}{\lambda_1} \cdot \left(1 + \frac{\delta_P}{\delta_C} \cdot \frac{\lambda_1}{Y_1 \beta_1 \eta_1} \right)$, which can be rewritten as

$$\frac{\eta_1 - \eta_2}{\frac{\lambda_2}{\lambda_1} \eta_1 - \eta_2} > \frac{\frac{\lambda_1}{Y_1 \beta_1 \eta_1} + \frac{\delta_C}{\delta_P}}{\frac{\lambda_2}{Y_2 \beta_2 \eta_2} + \frac{\delta_C}{\delta_P}} \qquad . \tag{16}$$

In the opposite limit of this inequality and for nutrient supply rates satisfying $\phi^{(2)} < \phi < \phi_{P1}$ the phages will be absent in one of the two alternative stable states (dominated by the species 1) but present in another one (dominated by the species 2).

The scenario illustrated in Fig . 2 corresponds to $\phi_{P1} < \phi^{(2)} < \phi^{(1)}$. In this case, the

abundances in the steady state S dominated by the fast growing species 1 are given by

$$B_1^{(F)} = \frac{\delta}{\beta_1 \eta_1} \tag{17}$$

$$B_2^{(F)} = 0 \tag{18}$$

$$C^{(F)} = \frac{\phi}{\delta + \lambda_1 B_1^{(F)}/Y_1} \tag{19}$$

$$P^{(F)} = \frac{\lambda_1 C^{(F)} - \delta}{\eta_1} \,. \tag{20}$$

The abundances in the alternative stable state F dominated by the slow growing species 2

$$B_1^{(S)} = 0 \tag{21}$$

$$B_2^{(S)} = \frac{\delta}{\beta_1 \eta_1} \tag{22}$$

$$C^{(S)} = \frac{\phi}{\delta + \lambda_2 B_2^{(S)}/Y_2} \tag{23}$$

$$P^{(S)} = \frac{\lambda_2 C^{(S)} - \delta}{\eta_2} \tag{24}$$

in the state dominated by the species 2.

In the regime where $\phi_{P1} < \phi^{(2)} < \phi^{(1)}$ and for nutrient supply rates in the bistable window $\phi^{(2)} < \phi < \phi^{(1)}$, the ecosystem also has a dynamically unstable steady state in which both bacterial species co-exists with each other and have the following abundances:

$$B_1^{(U)} = \frac{\delta}{\beta_1 \eta_1} \cdot \frac{\phi - \phi^{(2)}}{\phi^{(1)} - \phi^{(2)}} \tag{25}$$

$$B_2^{(U)} = \frac{\delta}{\beta_2 \eta_2} \cdot \frac{\phi^{(1)} - \phi}{\phi^{(1)} - \phi^{(2)}} \tag{26}$$

Note that in our study we consider only uninvadable states of the ecosystem. In other words, we ignore an invadable steady state, where for a small value of ϕ the ecosystem is populated only by the species 2, or another invadable steady state realized for a large value of ϕ, where the ecosystem has only the species 1. These states are located on invadable parts of each species' ZNGI, which are to the right and below the ZNGI of the other species in Fig. 4A. Indeed, in these regions an arbitrary small inoculum of the invading species would exponentially grow and thereby disrupt the steady state of the ecosystem moving the environmental variables to a new point on the (C, P) plane.

Parameters used in our numerical simulations Both in stochastic and deterministic simulations of our model shown in Figures (1-3) we used the following parameters:

$$\lambda_1 = 1.0; \quad \lambda_2 = 0.8 \tag{27}$$

$$Y_1 = 1; \quad Y_2 = 1 \tag{28}$$

$$\eta_1 = 0.2; \quad \eta_2 = 0.15 \tag{29}$$

$$\beta_1 = 2; \quad \beta_2 = 40 \tag{30}$$

$$\delta_C = \delta_B = \delta_P = 0.2 \,. \tag{31}$$

For these parameters the ecosystem is bistable when nutrient supply rate is between

$$\phi^{(2)} = 0.2266 \tag{32}$$

$$\phi^{(1)} = 0.7 \tag{33}$$

The bacterial abundances anywhere within this interval of nutrient supply rates are given by $B_1^{(F)} = 0.5$, $B_2^{(F)} = 0$ or $B_1^{(S)} = 0$, $B_2^{(S)} = 0.0333$ in alternative stable states dominated respectively by the fast and the slow-growing bacterial species.

The other transitions visible in Figure 2 happen at $\phi_{B1} = 0.04$ above which the bacterial species 1 is able to survive given the dilution rate δ, and $\phi_{P1} = 0.14$, above which the phage can survive in this ecosystem.

To estimate the typical values of C and P in two bistable states let us consider one example when $\phi = 0.25$ is slightly above $\phi_{(2)}$. In this case the steady state concentrations of the nutrient and the phage in two alternative stable states: F and S are given by

$$C^{(F)} = 0.357; \quad C^{(S)} = 1.277 \tag{34}$$

$$P^{(F)} = 0.786; \quad P^{(S)} = 5.476 \tag{35}$$

The dynamically unstable steady state point always has $C^* = 1$ and $P^* = 4$, which are located between their values in the F and S states. The bacterial abundances in an unstable state for $\phi = 0.25$ are given by $B_1^{(U)} = 0.0246$ and $B_2^{(U)} = 0.0317$. Note that the steady state abundance of the species 1 in the unstable state is much lower than its abundance $B_1^{(F)} = 0.5$ in the stable state. That suggests why for such a low value of ϕ we found it impossible to switch the ecosystem from the F state to the S state by pulses of C, P, or B_2. Indeed, neither of these transient pulses is capable of lowering down B_1 to the extra low saddle point value $B_1^{(U)} = 0.0246$ from initial stable state value of $B_1^{(F)} = 0.5$ without simultaneously moving the populations of other species away from the saddle point region.

The position of the crosses in Fig. 4A can be calculated as follows: at $\phi = \phi^{(1)} = 0.7$ the species 1 sets the environmental parameters of the ecosystem exactly at the intersection point $(C^*, P^*) = (1, 4)$ between ZNGIs of species 1 and 2. For slightly higher nutrient supply rates the species 2 eliminates the species 1 and the nutrient concentration shifts to $C_{2x} = \frac{\phi^{(1)}}{\delta_C + \delta_P \lambda_2/(Y_2 \beta_2 \eta_2)} = 3.09$, and the phage population - to $P_{2x} = (\lambda_2 C_{2x} - \delta_B)/\eta_2 = 15.14$. On the way down the bacterial species 1 reenters the ecosystem slightly below $\phi = \phi^{(2)} = 0.2266$. When the species 1 replaces the species 2 immediately below this point the nutrient concentration shifts to $C_{1x} = \frac{\phi^{(2)}}{\delta_C + \delta_P \lambda_1/(Y_1 \beta_1 \eta_1)} = 0.3238$, and the phage population - to $P_{1x} = (\lambda_1 C_{1x} - \delta_B)/\eta_1 = 0.6190$.

ACKNOWLEDGMENTS

REFERENCES

1. **Scheffer M, Carpenter SR.** 2003. Catastrophic regime shifts in ecosystems: linking theory to observation. Trends ecology & evolution 18(12):648–656.

2. **Gonze D, Lahti L, Raes J, Faust K.** 2017 10. Multi-stability and the origin of microbial community types. The ISME Journal 11(10):2159–2166. https://doi.org/10.1038/ismej.2017.60.

3. **Wright ES, Vetsigian KH.** 2016 4. Inhibitory interactions promote frequent bistability among competing bacteria. Nature Communications 7:11274. https://doi.org/10.1038/ncomms11274.

4. **Dubinkina V, Fridman Y, Pandey P, Maslov S.** 2018. Alternative stable states in a model of microbial community limited by multiple essential nutrients. arXiv preprint arXiv:1810.04726 .

5. **Goyal A, Dubinkina V, Maslov S.** 2018. Multiple stable states in microbial communities explained by the stable marriage problem. The ISME journal 12(12):2823.

6. **Thingstad T, Lignell R.** 1997. Theoretical models for the control of bacterial growth rate, abundance, diversity and carbon demand. Aquatic Microbial Ecology 13(1):19–27.

7. **Thingstad TF.** 2000. Elements of a theory for the mechanisms controling abundance, diversity, and biogeochemical role of lytic bacterial viruses in aquatic systems. Limnol. Oceanogr. 45:1320–1328.

8. **Gause GF.** 1932. Experimental studies on the struggle for existence: I. Mixed population of two species of yeast. Journal experimental biology 9(4):389–402.

9. **AM C.** 1960. Conditions for the existence of bacteriophage. Evolution 15:153–165.

10. **Haerter JO, Mitarai N, Sneppen K.** 2014. Phage and bacteria support mutual diversity in a narrowing staircase of coexistence. The ISME journal 8(11):2317.

11. **Hsu BB, Gibson TE, Yeliseyev V, Liu Q, Lyon L, Bry L, Silver PA, Gerber GK.** 2019 6. Dynamic Modulation of the Gut Microbiota and Metabolome by Bacteriophages in a Mouse Model. Cell Host Microbe https://doi.org/10.1016/j.chom.2019.05.001.

12. **Angulo MT, Moog CH, Liu YY.** 2019. A theoretical framework for controlling complex microbial communities. Nature communications 10.

13. **Chopin MC, Chopin A, Bidnenko E.** 2005. Phage abortive infection in lactococci: variations on a theme. Current Opinion Microbiology 8.

14. **Tilman D.** 1982. Resource competition and community structure. Princeton university press.

15. **Pfeiffer T, Schuster S, Bonhoeffer S.** 2001. Cooperation and Competition in the Evolution of ATP-Producing Pathways. Science 292(5516):504–507.

16. **Haerter JO, Mitarai N, Sneppen K.** 2016. Food web assembly rules for generalized Lotka-Volterra equations. PLoS computational biology 12(2):e1004727.

17. **Haerter JO, Mitarai N, Sneppen K.** 2017. Existence and construction of large stable food webs. Physical Review E 96(3):032406.

18. **Goh B.** 1977. Global Stability in Many-Species Systems. The American Naturalist 111:135–143.

19. **Lindeman RL.** 1942. The trophic-dynamic aspect of ecology. Ecology 23(4):399–417.

20. **Colinvaux P, Barnett B.** 1979. Lindeman and the ecological efficiency of wolves. The American Naturalist 114(5):707–718.

21. **Weitz JS, Dushoff J.** 2008. Alternative stable states in host–phage dynamics. Theoretical Ecology 1(1):13–19.

22. **Herskowitz I, Hagen D.** 1980. The lysis-lysogeny decision of phage lambda: explicit programming and responsiveness. Annual review genetics 14(1):399–445.

23. **Toman Z, Dambly-Chaudière C, Tenenbaum L, Radman M.** 1985. A system for detection of genetic and epigenetic alterations in Escherichia coli induced by DNA-damaging agents. Journal Molecular Biology 186:97–105.

24. **Reichardt L, Kaiser AD.** 1971. Control of λ Repressor Synthesis. Proc Natl Acad Sci USA 68:2185–2189.

25. **Eisen H, Brachet P, da Silva LP, Jacob F.** 1970. Regulation of Repressor Expression in λ. Proc. Natl Acad. Sci. USA 66:855–862.

26. **Kourilsky P.** 1973. Lysogenization by bacteriophage lambda. Molecular General Genetics MGG 122(2):183–195.

27. **Deveau H, Barrangou R, Garneau J, Labonté J, Fremaux C, Boyaval P, Romero D, Horvath P, Moineau S.** 2007. Phage Response to CRISPR-Encoded Resistance in Streptococcus thermophilus. J Bacteriol 190(4):1390–1400.

28. **Strotskaya A, Savitskaya E, Metlitskaya A, Morozova N, Datsenko KA, Semenova E, Severinov K.** 2017 2. The action of Escherichia coli CRISPR–Cas system on lytic bacteriophages with different lifestyles and development strategies. Nucleic Acids Research 45(4):1946–1957. https://doi.org/10.1093/nar/gkx042.

29. **Watson BN, Vercoe RB, Salmond GP, Westra ER, Staals RH, Fineran PC.** 2019. Type I-F CRISPR-Cas resistance against virulent phage infection triggers abortive infection and provides population-level immunity. bioRxiv p. 679308.

30. **Bohannan BJ, Lenski RE.** 2000. The relative importance of competition and predation varies with productivity in a model community. The American Naturalist 156(4):329–340.

31. **Labrie SJ, Samson JE, Moineau S.** 2010. Bacteriophage resistance mechanisms. Nature Reviews Microbiology 8:317.

32. **Levin BR, Stewart FM, Chao L.** 1977. Resource-Limited Growth, Competition, and Predation: A Model and Experimental Studies with Bacteria and Bacteriophage. The American Naturalist 111:3–24.